Recent Results on Four-loop Tadpoles

K. G. Chetyrkin[a*], J. H. Kühn[a] and C. Sturm[b]

[a]Institut für Theoretische Teilchenphysik, Universität Karlsruhe, D-76128 Karlsruhe, Germany

[b]Dipartimento di Fisica Teorica, Università di Torino, I-10125 Torino, Italy & INFN, Sezione di Torino

The experimental measurable R-ratio can be used to perform a precise determination of the charm- and bottom-quark mass with the help of theoretical computable expansion coefficients of the vacuum polarization function. The four-loop contributions in perturbative QCD to the first two expansion coefficients of the vacuum polarization functions are presented.

1. Introduction

Due to the progress in the last years in calculational techniques a number of physical quantities related to the computation of four-loop tadpole diagrams have been evaluated recently. For example, the matching condition for the strong coupling constant α_s at a heavy quark threshold has been determined in ref. [1,2] to four-loop order in the modified minimal subtraction scheme. This requires the calculation of tadpole diagrams with massive and massless propagators. The calculation of the four-loop β-function, which in contrast requires the evaluation of completely massive tadpole integrals, has been performed previously in ref. [3–5].

Moments of the cross section for electron-positron annihilation into hadrons are also related to tadpole diagrams. In this context the correlator of two electromagnetic currents $j^\mu(x) = \overline{\Psi}(x)\gamma^\mu\Psi(x)$ of a heavy quark with mass m_q is important. It is connected to the vacuum polarization function $\Pi(q^2)$ through:

$$(q^\mu\, q^\nu - q^2\, g^{\mu\nu})\,\Pi(q^2) = i\int dx e^{iqx}\langle 0|Tj^\mu(x)j^\nu(0)|0\rangle,$$

where q^μ is the external momentum. On the one hand the vacuum polarization function can be linked to moments $\mathcal{M}_n$ with the help of dispersion relations:

$$\mathcal{M}_n^{\exp} = \int ds \frac{R(s)}{s^{n+1}} = \frac{12\pi^2}{n!}\left(\frac{d}{dq^2}\right)^n \Pi(q^2)\Big|_{q^2=0},\quad(1)$$

$\mathcal{M}_n^{\exp}$ depends on the experimental measurable R-ratio $R(s) = \sigma(e^+e^- \to \text{hadrons})/\sigma(e^+e^- \to \mu^+\mu^-)$. On the other hand the derivatives of the vacuum polarization function can be calculated in perturbative QCD. Let us define

$$\overline{\Pi}(q^2) = \frac{3\,Q_q^2}{16\pi^2}\sum_{n\geq 0}\overline{C}_n\, z^n\,,\qquad(2)$$

where $z = q^2/(4\,\overline{m}_q^2)$ and Q_q is the electric charge of the heavy quark. For quantities with a bar renormalization is performed in the $\overline{\text{MS}}$-scheme. The expansion in equation (2) leads to tadpole integrals. From the first and the dhigher derivatives of the vacuum polarization function one can extract the heavy quark mass by combining equation (1) and (2):

$$\overline{m}_q(\mu) = \frac{1}{2}\left(\frac{9\,Q_q^2\,\overline{C}_n}{4\,\mathcal{M}_n^{\exp}}\right)^{1/(2\,n)}.\qquad(3)$$

This method has been originally used to determine the charm- and later the bottom-quark mass [6,7]. Taking into account moments up to three-loop order [8,9] precise results for both quark masses have been obtained [10,11]. In view of the present and foreseeable precision of experimental data it is important to know the four-loop

*On leave from Institute for Nuclear Research of the Russian Academy of Sciences, Moscow, 117312, Russia.

contributions [12] whose evaluation is subject of this work.

This article is structured as follows: In section 2 we outline the computation of the four-loop contributions to the vacuum polarization function in the low energy limit. We discuss the calculational methods, the determination of the master integrals and finally present the result. In section 3 we examine the phenomenological implications of this result and in section 4 we close with a brief summary and conclusions.

2. Outline of the calculation

Calculation methods

In a first step about 700 Feynman diagrams were generated using the program `QGRAF` [13] and classified according to the number of inserted closed fermion loops. In four-loop approximation one thus obtains three classes of diagrams for the considered problem, shown on fig. 1(a)-(c). Within this work we consider the calculation of the non-singlet diagrams at four-loop order. Contributions of singlet type diagrams like the representative in fig. 1(d) were studied in ref. [14–16].

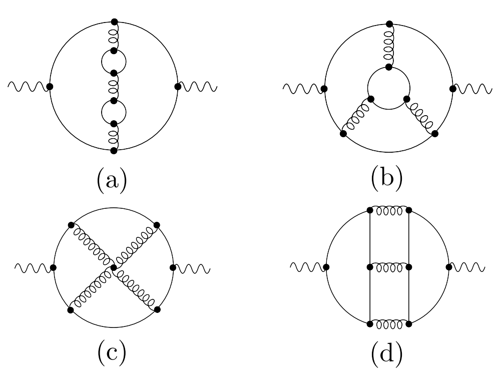

Figure 1. The first diagram (a) belongs to the n_f^2-contribution, the second diagram (b) to the n_f^1-contribution, the third diagram (c) contributes to the n_f^0-contribution, which does not involve any insertion of closed fermion loops. The fourth diagram (d) is a singlet-diagram. The wavy lines denote the external vector current and the spiral lines represent gluons.

The multitude of tadpole integrals have been reduced to a small set of master integrals with the traditional Integration-by-parts (IBP) method in combination with the Laporta-algorithm [17,18]. The generation and solution of the linear system of equations has been implemented in a program [19] based on `FORM`[20–22] and `FERMAT`[23], which is used to simplify the rational functions in the space time dimension d. Furthermore, all symmetries of the Feynman integrals have been taken into account in an automated way. This helps to reduce the number of initial IBP-identities, which need to be generated and solved. Likewise, the consideration of symmetries is important to keep the size of the integral tables containing the solutions of the linear system of equations under control. All integrals can thus be mapped on a small set of 13 master integrals.

Master integrals

The 13 master integrals have been evaluated in ref. [24] with the help of the difference equation method [18,17,25]. Independently they have been calculated in ref. [26] by constructing an ε-finite basis of master integrals.

While solving the system of IBP-identities a division by $\varepsilon = (4-d)/2$ can appear. The coefficient functions of the master integrals can contain so called spurious poles. Master integrals with spurious poles in their coefficient functions need to be evaluated deeper in the ε-expansion. In general each additional order in ε in which a master integral has to be evaluated is increasingly cumbersome, in particular, if numerical methods need to be applied. For this reason it is useful to select a set of master integrals whose coefficient functions are finite in the limit $\varepsilon \to 0$ by exploiting the freedom in the choice of the master integrals. This defines an ε-finite basis. Trivial master integrals, which can be completely expressed in terms of Γ-function, are not considered in this construction. These are shown in fig. 2.

For the remaining nine master integrals an ε-finite basis has been constructed in ref. [26]. The master integrals are shown in fig. 3. The ε-finite master integrals have been calculated semi-numerically in ref. [26] with the help of Padé approximations [27–30]. The result is in perfect agreement with ref. [24].

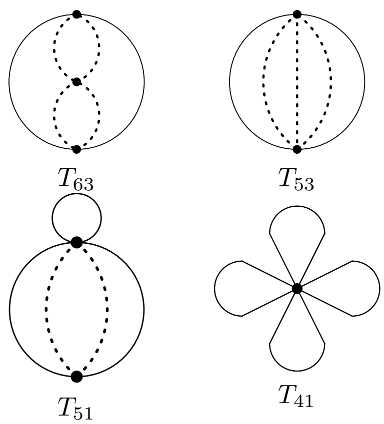

Figure 2. Master integrals which are known completely analytically. The solid (dashed) lines denote massive (massless) propagators.

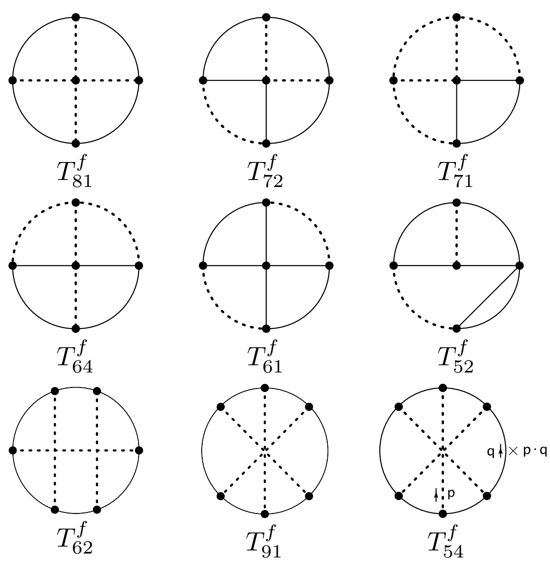

Figure 3. Master integrals being member of the ε-finite basis. The solid (dashed) lines denote massive (massless) propagators. One master integral (T^f_{54}) has a scalar product.

Result

If ones inserts the results for the master integrals into the solution provided by the Laporta-algorithm and performs renormalization in the $\overline{\rm MS}$-scheme one obtains for the first two expansion coefficients $\overline{C}_0$ and $\overline{C}_1$ (adopting the renormalization scale $\mu = m$):

$$\begin{aligned}\overline{C}_0 \;=\; &+\left(\frac{\alpha_s}{\pi}\right)\; 1.44444444444444 \\ &+\left(\frac{\alpha_s}{\pi}\right)^2 \big(1.72492329642573 \\ &\qquad +0.37139917695473\, n_l\big) \\ &+\left(\frac{\alpha_s}{\pi}\right)^3 \big(-1.95490692882665 \\ &\qquad -1.18600984426309\, n_l \\ &\qquad +0.02570664656045\, n_l^2\big)\,, \end{aligned} \qquad (4)$$

$$\begin{aligned}\overline{C}_1 \;=\; &+1.06666666666667 \\ &+\left(\frac{\alpha_s}{\pi}\right)\; 2.55473251028807 \\ &+\left(\frac{\alpha_s}{\pi}\right)^2 \big(0.50988169828765 \\ &\qquad +0.66227709190672\, n_l\big) \\ &+\left(\frac{\alpha_s}{\pi}\right)^3 \big(1.87882284654395 \\ &\qquad -2.79472185790743\, n_l \\ &\qquad +0.09610140043295\, n_l^2\big)\,. \end{aligned} \qquad (5)$$

The symbol n_l denotes the number of light active quarks which are considered as massless. The n_f^2-contribution[31] and n_f^1-contribution are known completely analytically. The terms proportional to $\alpha_s^k\, n_l^{k-1}$ are known to all orders k in [32]. The results for $\overline{C}_0$ and $\overline{C}_1$ in the analytical form are given in [12].

3. Phenomenological implications

In this section we discuss the influence of the newly computed correction on the charm- and bottom-quark masses as well as its effect on the (unphysical) renormalization scale dependence of the scale-invariant quark masses. In our analysis we will closely follow [10]. In particular, we will take from [10] the value of the first "experimental" moment as defined in eq. (1). The latest experimental information on $R(s)$ which appeared after publication of [10] will be taken into account in a future study.

Using relation (3) for the first moment at three- and four-loop approximations one can assess the influence of the new four-loop order on the values of the charm- and bottom-quark mass.

Let us first summarize the current status of the charm- and bottom-quark masses as obtained in [10] from the first moment evaluated to order α_s^2:

$$\overline{m}_c(3\,\text{GeV}) = 1.027 \pm 0.002\,\text{GeV}, \quad (6)$$
$$\overline{m}_b(10\,\text{GeV}) = 3.665 \pm 0.005\,\text{GeV}. \quad (7)$$

Note that here and below we display only the uncertainties coming from the variation of the renormalization scale μ in the region $\mu = 10 \pm 5\,\text{GeV}$ for the bottom-quark and $\mu = 3 \pm 1\,\text{GeV}$ for the charm-quark respectively. The transformation of the results to the scale invariant mass $\overline{m}_q(\overline{m}_q)$ using the *three-loop coefficients* of the renormalization group (RG) functions leads to

$$\overline{m}_c(\overline{m}_c) = 1.304 \pm 0.002\,\text{GeV}, \quad (8)$$
$$\overline{m}_b(\overline{m}_b) = 4.205 \pm 0.005\,\text{GeV}. \quad (9)$$

The inclusion of the four-loop contribution to the function $\overline{C}_1$ leads for the case of the charm-quark to the following modification of eq. (6):

$$\overline{m}_c(3\,\text{GeV}) = 1.023^{+0.00005}_{-0.0005}\,\text{GeV}, \quad (10)$$

which corresponds to the following result for the scale-invariant mass:

$$\overline{m}_c(\overline{m}_c) = 1.310^{+0.00004}_{-0.0004}\,\text{GeV}. \quad (11)$$

Note that for both equations above we have used the evolution with four-loop accuracy as required by the self-consistency considerations. If we would use the RG equation only with the three-loop accuracy this would not only lead to somewhat larger errors (by around 20-25%) but also to a *significantly smaller* value of $\overline{m}_c(\overline{m}_c) = 1.300\,\text{GeV}$.

For the case of the bottom-quark our results read:

$$\overline{m}_b(10\,\text{GeV}) = 3.665^{+0.0002}_{-0.0011}\,\text{GeV}, \quad (12)$$

which corresponds to the following result for the scale-invariant mass:

$$\overline{m}_b(\overline{m}_b) = 4.210^{+0.0002}_{-0.0011}\,\text{GeV}. \quad (13)$$

Again the equations above correspond to the use of the four-loop evolution equation. Due to the larger scale involved the use of the three-loop running would move the $\overline{m}_b(\overline{m}_b)$ by about five MeV down (leaving it practically unchanged from the result of [10] within our accuracy) and again would lead to a slight increase of the error.

4. Summary and conclusion

The calculation of the expansion coefficients of the vacuum polarization function allows a precise determination of the charm- and bottom-quark masses. The reduction to master integrals of the first two expansion coefficients $\overline{C}_0$ and $\overline{C}_1$ at four-loop order in perturbative QCD has been completed using the IBP-method in combination with the Laporta-Algorithm. Furthermore all master integrals were obtained with two independent methods: the difference equation method and the method of the ε-finite basis. The influence of the new four-loop contributions on the values of the charm- and bottom-quark mass is small: the newly computed four-loop term moves up the charm-quark mass by 6 MeV and the bottom-quark mass by 5 MeV.

Acknowledgments:
The authors are grateful to M. Faisst for numerous discussions and for providing numerical cross checks of partial results. We thank M. Czakon for an interesting discussion. The work was supported by the Deutsche Forschungsgemeinschaft through the SFB/TR-9 “Computational Particle Physics”. The work of C.S. was also partially supported by MIUR under contract 2001023713_006.

Note added.
The results of our calculations as expressed in eq. (5) have been confirmed in the work [33], where also a strong reduction of the theoretical error due to the unphysical scale dependence of $\overline{m}_q(\overline{m}_q)$ has been found. Furthermore, the complete four-loop QCD correction to the electroweak ρ parameter were calculated in [34] and confirmed in [35] (note that the calculation of the so-called singlet contribution to the full result was performed in an earlier work [36]).

REFERENCES

1. Y. Schröder and M. Steinhauser, JHEP 01 (2006) 051, hep-ph/0512058.
2. K.G. Chetyrkin, J.H. Kühn and C. Sturm, Nucl. Phys. B744 (2006) 121, hep-ph/0512060.
3. T. van Ritbergen, J.A.M. Vermaseren and S.A. Larin, Phys. Lett. B400 (1997) 379, hep-ph/9701390.
4. K. Kajantie et al., JHEP 04 (2003) 036, hep-ph/0304048.
5. M. Czakon, Nucl. Phys. B710 (2005) 485, hep-ph/0411261.
6. V.A. Novikov et al., Phys. Rept. 41 (1978) 1.
7. L.J. Reinders, H. Rubinstein and S. Yazaki, Phys. Rept. 127 (1985) 1.
8. K.G. Chetyrkin, J.H. Kühn and M. Steinhauser, Nucl. Phys. B482 (1996) 213, hep-ph/9606230.
9. K.G. Chetyrkin, J.H. Kühn and M. Steinhauser, Nucl. Phys. B505 (1997) 40, hep-ph/9705254.
10. J.H. Kühn and M. Steinhauser, Nucl. Phys. B619 (2001) 588, hep-ph/0109084.
11. J.H. Kühn and M. Steinhauser, JHEP 10 (2002) 018, hep-ph/0209357.
12. K.G. Chetyrkin, J.H. Kühn and C. Sturm, (2006), hep-ph/0604234.
13. P. Nogueira, J. Comput. Phys. 105 (1993) 279.
14. S. Groote and A.A. Pivovarov, Eur. Phys. J. C21 (2001) 133, hep-ph/0103313.
15. J. Portoles and P.D. Ruiz-Femenia, J. Phys. G29 (2003) 349, hep-ph/0107324.
16. J. Portoles and P.D. Ruiz-Femenia, Eur. Phys. J. C24 (2002) 439, hep-ph/0202114.
17. S. Laporta, Int. J. Mod. Phys. A15 (2000) 5087, hep-ph/0102033.
18. S. Laporta and E. Remiddi, Phys. Lett. B379 (1996) 283, hep-ph/9602417.
19. C. Sturm, PhD thesis, Cuvillier Verlag, Goettingen ISBN 3-86537-560-X (2005) , .
20. M. Tentyukov and J.A.M. Vermaseren, Extension of the functionality of the symbolic program FORM by external software, cs.sc/0604052 (2006).
21. J.A.M. Vermaseren, Nucl. Phys. Proc. Suppl. 116 (2003) 343, hep-ph/0211297.
22. J.A.M. Vermaseren, New features of FORM, math-ph/0010025 (2000) .
23. R.H. Lewis, Fermat's User Guide, http://www.bway.net/~lewis/ .
24. Y. Schröder and A. Vuorinen, JHEP 06 (2005) 051, hep-ph/0503209.
25. S. Laporta, Phys. Lett. B549 (2002) 115, hep-ph/0210336.
26. K.G. Chetyrkin et al., Nucl. Phys. B742 (2006) 208, hep-ph/0601165.
27. J. Fleischer and O.V. Tarasov, Z. Phys. C64 (1994) 413, hep-ph/9403230.
28. P.A. Baikov and D.J. Broadhurst, (1995), hep-ph/9504398.
29. M. Faisst, K.G. Chetyrkin and J.H. Kühn, Nucl. Phys. Proc. Suppl. 135 (2004) 307.
30. M. Faisst, PhD thesis, Cuvillier Verlag, Goettingen ISBN 3-86537-506-5 (2005) , .
31. K.G. Chetyrkin et al., Eur. Phys. J. C40 (2005) 361, hep-ph/0412055.
32. A.G. Grozin and C. Sturm, Eur. Phys. J. C40 (2005) 157, hep-ph/0412040.
33. R. Boughezal, M. Czakon and T. Schutzmeier, (2006), hep-ph/0605023.
34. K.G. Chetyrkin et al., (2006), hep-ph/0605201.
35. R. Boughezal and M. Czakon, (2006), hep-ph/0606232.
36. Y. Schröder and M. Steinhauser, Phys. Lett. B622 (2005) 124, hep-ph/0504055.